AJNR

This information is current as of May 12, 2025.

CSF Leaks: Correlation of High-Resolution CT and Multiplanar Reformations with Intraoperative Endoscopic Findings

V. La Fata, N. McLean, S.K. Wise, J.M. DelGaudio and P.A. Hudgins

ORIGINAL RESEARCH

V. La Fata
N. McLean
S.K. Wise
J.M. DelGaudio
P.A. Hudgins

CSF Leaks: Correlation of High-Resolution CT and Multiplanar Reformations with Intraoperative Endoscopic Findings

BACKGROUND AND PURPOSE: Skull base defects can result in CSF leaks, with meningitis as a potential complication. Surgeons are now routinely repairing these leaks via a nasal endoscopic approach. Accurate preoperative imaging is essential for surgical planning. A variety of imaging regimens have been employed, including axial and direct coronal CT, CT cisternography with iodinated contrast, radionuclide cisternography, and MR imaging. Now that multidetector helical CT is available, the purpose of this study was to determine how well coronal and sagittal multiplanar reformatted (MPR) images generated from a high-resolution axial dataset correlate with intraoperative findings in a group of patients with clinically proved CSF leaks.

MATERIALS AND METHODS: We retrospectively reviewed imaging findings and surgical records of 19 patients who presented to our tertiary care institution during a 2.5-year period with clinically proved CSF leak. Patients underwent preoperative imaging with high-resolution helical CT (section collimation, 10 patients with 0.625-mm and 9 patients with 1.25-mm images), with MPR images processed by a neuroradiologist at a workstation. Two neuroradiologists, blinded to the intraoperative findings, determined the location and size of the skull base defects. All patients underwent endoscopic evaluation by an experienced sinonasal otolaryngologist, who confirmed the site of the CSF leak by direct inspection and measured the corresponding osseous defect. CT was considered accurate if it correctly localized the CSF leak and was within 2 mm of the endoscopic measurement.

RESULTS: At endoscopy, 22 leaks of CSF were identified in 18 of 19 patients. CT correctly predicted the site of the leak in 20 (91%) of 22 cases and was accurate (within 2 mm of the endoscopic measurement) in 15 (75%) of 20 cases preoperatively localized. The CT measurement of the skull base defect differed from the endoscopic size in 5 (25%) of 20 cases, ranging from 7.4 mm below to 13 mm above the intraoperative measurement. When analysis was limited to the subgroup of 10 patients who had 0.625-mm axial images, the accuracy was improved, and of the 11 CSF leaks described at CT, all were verified at endoscopy. In addition, the submillimeter CT accurately measured the size of the osseous defect in 9 (82%) of 11 cases. In the remaining 2 (18%) of 11 cases, CT minimally overestimated the size of the osseous defect by only 3 mm.

CONCLUSION: Axial images, and coronal, sagittal, and oblique MPR images generated from high-resolution axial CT performed well preoperatively, localizing the skull base defect responsible for the CSF leak. However, active manipulation of the axial dataset at a workstation is crucial in identifying and correctly describing these lesions. When submillimeter collimation is available, measurement of the osseous defects are accurate most of the time.

Skull base defects that result in dural tears and CSF leaks can be associated with significant long-term disability, primarily related to central nervous system infection. Bacterial meningitis is the major cause of morbidity and mortality, with encephalitis and parenchymal abscess occurring much less frequently[1]. Left untreated, some may resolve spontaneously, but the risk for meningitis is 10% annually and up to 40% in the long term.[2] CSF leaks occur in approximately 2% of closed head injuries, the most common cause of CSF leak.[3] Other causes include a tumor or developmental malformations of the skull base, and surgical trauma. CSF leaks may also arise spontaneously, especially in the setting of idiopathic intracra-

nial hypertension. More than 90% of CSF leaks are successfully treated by minimally invasive intranasal endoscopic repair.[2,3] Even when CSF leaks cease spontaneously, early endoscopic repair is often considered because of a significant risk, estimated at 30% to 40%, for ascending meningitis.[3]

In patients with profuse posttraumatic or postsurgical CSF leaks, the diagnosis is obvious. However, in patients with intermittent CSF leaks that result in minimal discharge, the diagnosis may remain elusive. In this circumstance, beta2-transferrin (β_2-TF) assay provides a highly sensitive and specific (97% and 99%, respectively) method to confirm CSF leak.[4] β_2-TF protein is found almost exclusively in CSF, and as little as 0.5 mL of CSF is needed for the assay.[3] Once the clinical suspicion of CSF leak is confirmed with β_2-TF, the skull base defect responsible for the leak must be identified.

A variety of diagnostic modalities have been proposed for the preoperative localization of CSF leaks. In the traditional sense, CT and radionuclide cisternography have been the mainstays in the diagnostic evaluation, but their accuracy diminishes when CSF leaks are intermittent, a frequent occurrence. More recently, high-resolution CT without intrathecal

contrast and with the use of axial and direct coronal planes has been shown to reliably demonstrate skull base defects that result in CSF leaks.[5,6] With this technique, the skull base defect can be localized even when there is no active leak. Given that coronal images are essential in identifying skull base defects, the purpose of our study was to determine how well high-resolution coronal, sagittal, and oblique multiplanar reformatted (MPR) images generated from an axial dataset correctly predict the site of a CSF leak. It is perhaps more important to note that our series is the first, to our knowledge, to evaluate how accurately CT measurements compare with intraoperative sizes of the responsible skull base defects.

Methods

Imaging findings as well as the clinical and intraoperative data of 19 patients who underwent endoscopic repair for skull base defects during a 30-month period were retrospectively analyzed. Inclusion criteria required clinical suspicion for a CSF leak, preoperative CT imaging, and intraoperative exploration, with description of the location and size of any skull base defect. Patients with central skull base defects from tumors were excluded because the operative notes described only a "large" skull base defect. CSF leaks from temporal bone defects were not included because they are not repaired endoscopically.

CSF leaks were confirmed preoperatively in 17 patients with use of the β_2-TF assay of the clear rhinorrhea. All patients underwent noncontrast high-resolution multidetector row CT (MDCT) before undergoing surgery. Patients were scanned in the supine position. Ten patients were imaged on a 16-detector scanner, which generated 0.625-mm section collimation. A total of 9 patients were imaged on an 8-detector scanner, providing 1.25-mm section collimation. Scanning parameters were the same for both groups: 25-cm field of view, 512×512 matrix, and a bone reconstruction algorithm to enhance bony detail. The field of view included the sinonasal region and temporal bones to evaluate all potential sites of CSF leaks. Images were reconstructed with approximately 30% to 50% overlap. MPR images were generated and reviewed simultaneously with the axial dataset on a workstation.

Two neuroradiologists recorded the site and size of the skull base defect by consensus. The largest measurable defect obtained in the coronal, sagittal, oblique, or axial plane was reported. The CT images were interpreted without knowledge of the intraoperative findings; specifically, neither the presence, site, nor size of the leak was known at the time of image review. Positive CT criteria included an osseous defect in the skull base with associated mucosal thickening, soft tissue, or an air-fluid level in the adjacent sinonasal space. If the skull base was thinned but for a short segment, and there was no associated soft tissue on the nasal cavity side and no evidence for previous trauma or surgery at that location, the thinning was assumed to be normal. The cribriform plate was the most common place where the skull base appeared thin, but that was considered normal. CT was considered accurate if the findings correctly predicted the location of the CSF leak and the CT measurement was within 2 mm of the endoscopic defect measurement.

All patients were taken to surgery by a single experienced otolaryngologist. The preoperative CT directed the initial intraoperative endoscopic examination, but the skull base was carefully examined around the suspected leak site. The CSF leak was confirmed endoscopically by the presence of pooling CSF or a meningocele or meningoencephalocele. Once the leak was identified, the mucosa surround-

ing the skull base defect was completely stripped away to expose the entire osseous defect. The size of the skull base defect was measured with a surgical probe of known diameter. The largest size in a single dimension was recorded and compared with the maximum dimension reported on CT for the same location. Follow-up ranged from 2 weeks to 30 months (average, 6 months) in 18 of 19 patients, with cessation of CSF leaks in all patients who had clinical follow-up. Patient 15 had no clinical follow-up.

Results

The study group consisted of 2 men and 17 women (age range, 35–68 years; average, 48 years). Seventeen patients presented with a CSF leak that was preoperatively confirmed with β_2-TF. Of the 2 patients with no laboratory confirmation of a CSF leak, 1 presented with a known skull base defect after endoscopic sinus surgery (ESS), and 1 presented with a spontaneous encephalocele described on MR imaging. Among the 19 patients, 8 had spontaneous skull base defects, 9 had postsurgical defects (6/9 ESS, 2/9 transsphenoidal hypophysectomy, 1/9 craniotomy), 1 had a posttraumatic defect, and 1 had an iatrogenic defect (inadvertent nasogastric tube placement).

CT demonstrated 23 suspected skull base defects in 19 patients, ranging in size from 2 to 18 mm, with an average size of 6 mm. Endoscopy identified 22 CSF leaks in 18 of 19 patients. At endoscopy, there were 15 patients with a single site of a CSF leak, 2 patients with 2 separate sites, and 1 patient with 3 separate sites. A single patient had no leak identified at endoscopy, though CT showed 2 suspected 3-mm defects. Although initial results of β_2-TF in this patient were positive, results of repeat β_2-TF after negative endoscopy were also negative, and we speculate that the CSF leak healed spontaneously. The skull base defects ranged in size from 2 to 15 mm, with an average size of 6 mm.

CSF leaks detected on endoscopic examination occurred at 4 sites: 7 of 22 at the ethmoid, 7 of 22 at the sphenoid, 5 of 22 at the cribriform plate, and 3 of 22 in the posterior wall of the frontal sinus. The 8 spontaneous CSF leaks confirmed at endoscopy were distributed among the ethmoid roof (1/8), sphenoid (2/8), cribriform (3/8), and posterior wall of the frontal sinus (2/8). A total of 11 postsurgical CSF leaks in 9 patients, with the exception of a single leak at the cribriform plate, were evenly distributed between the ethmoid roof and sphenoid bone. The accompanying Table summarizes the imaging and clinical data.

Of the 22 CSF leaks confirmed at surgery, CT predicted the correct site in 20 (91%) (Fig. 1 and 2). Therefore, endoscopy identified only 2 small CSF leaks that were missed by CT, a 3-mm right cribriform plate defect (patient 12, Fig 3), and a 2-mm sphenoid defect (patient 10). In both of these patients, more than 1 site of a leak was detected on endoscopic examination, and CT correctly identified the other site of the CSF leak. Therefore, in the 2 patients who had leaks missed on CT, both had additional CSF leaks that were repaired endoscopically. In patient 12 were 2 separate leaks in the right cribriform plate. CT detected the larger 4-mm defect but missed a 3-mm defect that was seen on endoscopic examination. The 3-mm cribriform defect was found in retrospect once the intraoperative findings were revealed to the neuroradiologists. In patient 10 were 3 endoscopic defects in the sphenoid sinus, 2 of which were correctly located on CT. The third lesion could not

Imaging and clinical data on CSF leaks						
Patient No.	Cause	SC (mm)	CT Defect (mm)	Endo Defect (mm)	Accurate (± 2 mm)	Discrepancy (mm, Over/Under)
1	SP	1.2	R eth (6)	R eth (5)	Y	—
			L eth (6)	—	—	—
2	S	0.6	L eth (6)	L eth (6)	Y	—
3	SP	1.2	R sph (3)	—	—	—
			L eth (3)	—	—	—
4	SP	1.2	R fr p wall (13)	R fr p wall (15)	Y	—
5	SP	0.6	L sph (6)	L sph (6)	Y	—
6	S	0.6	R eth (5)	R eth (2)	N	3 over
7	S	0.6	Rt sph (3)	R sph (3)	Y	—
8	S	0.6	L eth (9)	L eth (10)	Y	—
9	S	1.2	L crib (7)	L crib (7)	Y	—
10	S	1.2	L sph (7)	L sph (14)	N	7 under
			R sph (3)	R sph (2)	Y	—
			—	R sph (2)	—	—
11	SP	1.2	L crib (12)	L crib (10)	Y	—
12	SP	0.6	R crib (5)	R crib (4)	Y	—
			—	R crib (3)	—	—
13	SP	0.6	L sph (2)	L sph (2)	Y	—
14	T	0.6	L eth (11)	L eth (10)	Y	—
			L fr p wall (3)	L fr p wall (3)	Y	—
15	S	0.6	R eth (6)	R eth (3)	N	3 over
16	S	1.2	R eth (18)	R eth (5)	N	13 over
17	SP	0.6	R fr p wall (6)	R fr p wall (8)	Y	—
18	I	1.2	L crib (8)	L crib (3)	N	5 over
19	S	1.2	L sph (5)	L sph (4)	Y	—

Note:—Endo indicates endoscopy; SP, spontaneous; S, surgical; T, traumatic; I, iatrogenic (other); p, posterior; eth, ethmoid; sph, sphenoid; fr, frontal; crib, cribriform; SC, slice collimation; L, left; R, right.
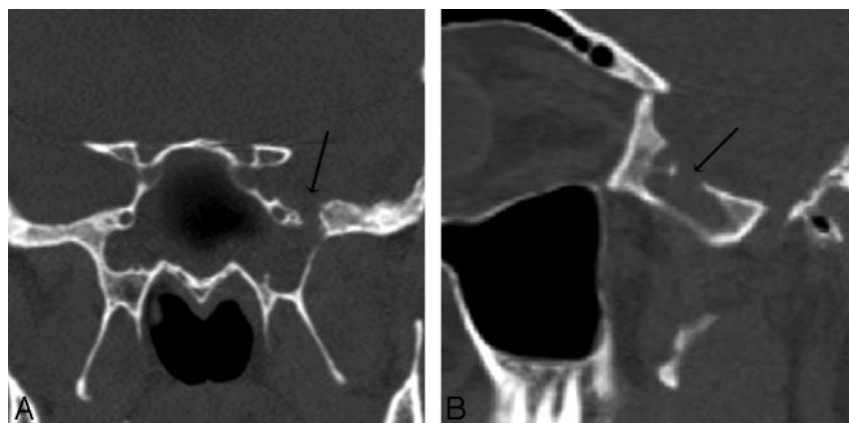

Fig 1. Patient 5. CT and endoscopy are concordant. Coronal (A) and oblique sagittal (B) MPR images generated from a 0.625-mm axial dataset demonstrate a 6-mm defect in a pneumatized pterygoid recess of the left sphenoid bone. There is mucosal thickening and an air-fluid level was present (other images) in the sphenoid sinus. At endoscopy, CSF was actively leaking at this site and the maximum size of the skull base defect (anteroposterior dimension), was identical to the CT measurement (6 mm).

be identified on CT even after the intraoperative findings were reported.

Of the 23 skull base defects described on CT, 20 (87%) were corroborated endoscopically. There were 3 of 23 skull base defects that were noted on CT but were not considered to be sites of a CSF leak at surgery. Patient 1 had 2 skull base defects noted on CT, only 1 of which was actively leaking CSF intraoperatively. In this case, the leaking defect at the right posterior ethmoid was accurately described on CT, but the left ethmoid defect was not leaking CSF intraoperatively. However, the left ethmoid defect noted on CT corresponded to a previously repaired spontaneous encephalocele, with an intracranial bone graft above the endoscopically verified skull base defect. Even in retrospect, the bone graft could not be identified on CT. In patient 3 were 2 separate skull base defects identified on CT. An air-fluid level was associated with the right sphenoid defect (Fig 4) and mucosal thickening with the

left ethmoid defect, but at endoscopy, no active CSF leak or bony defect was identified at either site. Results of a repeat β_2-TF in this patient were negative.

In the 20 defects in which CT correctly predicted the site of the CSF leak, the CT measurement was accurate in 15 (75%). In the remaining 5 (25%) cases, CT correctly located the CSF leak site but inaccurately measured the osseous defect, ranging from 7 mm below to 13 mm above the intraoperative measurement. When the analysis was limited to the 10 patients who had the 0.625-mm reconstructed axial images, rates of accuracy improved. Submillimeter CT identified 11 CSF leaks, all of which were corroborated intraoperatively. Of the 22 skull base defects, 15 (68%) were accurately measured on CT. Of the 5 cases considered to be inaccurate, CT overestimated the size of the skull base defect in 4 of 5 by an average of 6 mm (range, 3–l3 mm) (Fig 5). Submillimeter CT missed only 1 CSF leak, which was the 3-mm cribriform defect in patient 12 mentioned previously.

Fig 2. Patient 4. CT underestimates defect size by 2 mm. Sagittal MPR image from 1.25-mm axial dataset demonstrates a 13-mm defect in the posterior wall of the right frontal sinus with soft tissue suggestive of encephalocele protruding through the defect. At endoscopy, this was a 15-mm defect. MR was performed preoperatively and showed no encephalocele.
Fig 3. Patient 12. Both readers missed a defect found at endoscopy. Coronal MPR image from 0.625-mm axial dataset missed a subtle defect of the right cribriform plate, measuring 3 mm endoscopically and 2 mm by imaging. Two defects were present on the right in this patient; readers detected the first, but not the second, defect. In retrospect, a small amount of soft tissue or fluid attenuation extends medially along the horizontal insertion of the middle turbinate, or olfactory recess, through the skull base defect.
Fig 4. Patient 3. CT shows a defect but no CSF leak at endoscopy. Axial image from 1.25-mm axial dataset demonstrates a 3-mm defect in the right sphenoid bone. During endoscopy, after mucosa was elevated off the defect, no egress of CSF was seen from the defect.

Discussion

Until recently, CT cisternography has been considered the standard reference for preoperative evaluation of a CSF leak.[7] With this technique, contrast pooling in a sinus is considered to be a positive study. The ability of CT cisternography to accurately identify the culprit skull base defect depends on performing the procedure while CSF is actively leaking. Therefore, the overall sensitivity is poor because intermittent leaks will be missed. During active leaking, sensitivity approaches 92%, but it drops significantly to 40% when the CSF leak is intermittent.[7] CT cisternography carries some risk, albeit low, including infection, bleeding at the puncture site, and lumbar CSF leaks resulting in low-tension headaches. Another diagnostic technique used for CSF leaks is radionuclide cisternography, which also has a low sensitivity (62%–76%) and a false-positive rate of nearly 33%.[3] Furthermore, radionuclide cisternography typically localizes the leak to the right or left sinonasal space without precise subsite localization. Stone et al[8] directly compared noncontrast high-resolution CT with radionuclide cisternography and CT cisternography in 42 patients with CSF leaks.[8] The sensitivity of noncontrast high-resolution CT was greater than that of radionuclide cisternography and CT cisternography. In the subgroup of 21 patients who had surgical corroboration, the sensitivity of noncontrast high-resolution CT was 100% compared with 76% for radionuclide cisternography and 48% for CT cisternography. It is important to note that there were no positive radionuclide and CT cisternogram studies without previous positive identification of a skull base defect on noncontrast CT.

MR cisternography, typically consisting of multiplanar heavily T2-weighted sequences, is reported to be a highly sensitive and specific (85% and 100%, respectively) technique in localizing CSF leaks by demonstrating high signal intensity extending from the subarachnoid compartment into the sinonasal spaces.[7] Success with MR cisternography does not seem to be dependent on an active CSF leak but, like high-resolution CT, is an anatomic study. MR cisternography also identifies associated meningoencephaloceles and secondary parenchymal changes in signal intensity that reflect underlying CSF leaks, without exposing patients to lumbar puncture. However, MR cisternography does not provide the fine bony detail necessary for planning minimally invasive endoscopic repair. In our experience, all patients with positive results on a MR cisternogram, usually obtained after the CT scan to exclude a meningocele, have already had a high-resolution skull base CT for the surgical repair to be planned.

Shetty et al[7] compared high-resolution noncontrast CT and MR cisternography in the diagnosis of a CSF leak. The sensitivity, specificity, and accuracy of noncontrast CT cisternography were 92%, 100%, and 93%, respectively, and the sensitivity, specificity, and accuracy of noncontrast MR cisternography were 87%, 100%, and 89%, respectively.[7] Noncontrast CT and MR cisternography provided complementary information, with CT demonstrating the bone defect and MR, the leaking CSF column. As a result, the combined sensitivity, specificity, and accuracy improved to 95%, 100%, and 96%, respectively. Another important finding was that the accuracy of noncontrast CT was equally good in active and inactive CSF leaks.

CT protocols used to date[5,7,8] have used direct coronal images in addition to axial sections. The coronal plane has been necessary to completely evaluate the skull base because osseous defects in the ethmoid roof and planum sphenoidale are parallel to the scan plane and therefore are almost never apparent on axial sections. With recent developments of volumetric MDCT, high-resolution, essentially isotropic datasets can be acquired and, in turn, can be used to generate high-quality multiplanar images that can be viewed in any arbitrary plane.[9] It has been demonstrated that the image quality of coronal multiplanar reconstructions with 0.5-mm collimation, with or without overlapping reconstructions, is similar to that of contiguous direct coronal 0.5-mm sections.[10]

Our study is the first, to our knowledge, to show that high-resolution multiplanar images generated from a thin-collimation axial dataset reliably localize CSF leaks. Of the 22 leaks verified on endoscopic examination, MPR images correctly identified 20, a rate similar to that achieved with thin-section direct coronal CT.[7,8] The false-negative rate was also low. MPR
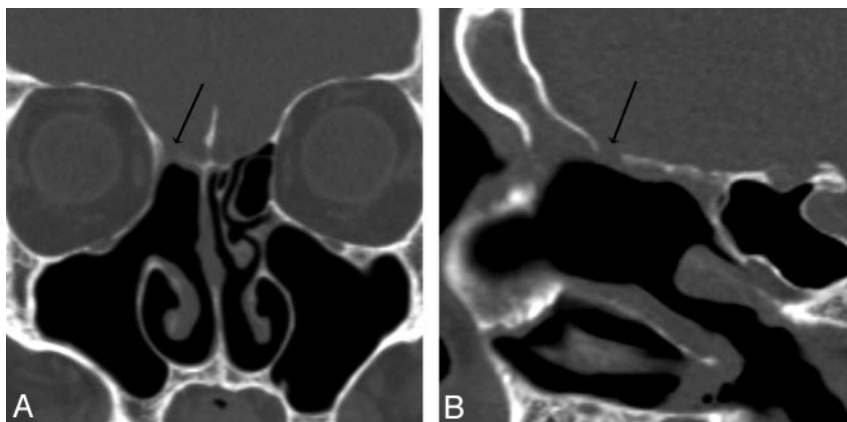
Fig 5. Patient 6. CT overestimated the size of the defect. Coronal (*A*) and sagittal (*B*) MPR images generated from a 0.625-mm axial dataset demonstrate a 5-mm defect in the right ethmoid roof. This patient has had a total ethmoidectomy, and the right middle turbinate has been resected at the skull base. There is mild mucosal thickening below the defect. At endoscopy, the CSF leak localized to this defect but measured only 2 mm.
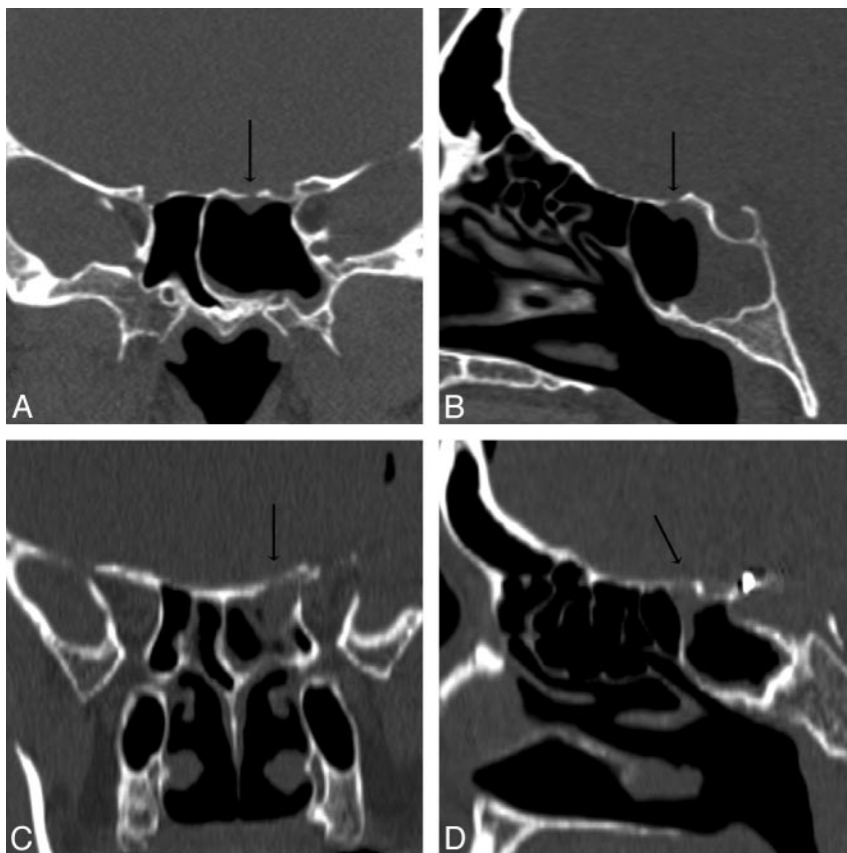

Fig 6. Patients 13 (*A and B*) and 19 (*C and D*). Coronal and sagittal MPR images in *A1* and *A2* and *B1* and *B2* are generated from 0.625-mm and 1.25-mm axial datasets, respectively. Although both of these MPR images resulted in accurate measurements of the CSF leaks, a 2.0-mm defect of the left sphenoid roof in patient 13 is better appreciated than the larger, 5.0-mm defect of the left sphenoid roof in patient 19 because of the overall improved resolution of submillimeter axial collimation.

images only missed 2 small lesions, both of which occurred in patients with additional larger CSF leaks. This highlights the fact that there may be multiple active CSF leaks, so careful scrutiny of the entire skull base is crucial even after 1 skull base defect is found. In patient 12 (Fig 3), minimal soft tissue below the osseous defect suggested the presence of a defect. Although subtle, we consider this an interpretive error rather than a failure of the technique.

The second goal of our study was to evaluate the accuracy of CT imaging in determining the size of skull base defects. To date, the literature has reported only on the ability of various imaging modalities to localize CSF leaks. However, knowledge of the size and configuration of a skull base defect provides useful information that facilitates presurgical planning, especially if the defect is large. Endoscopic repair of CSF leaks has a high rate of success and is currently the mainstay of repair of CSF leaks.[11-14]

Our series demonstrated that MPR images from 0.625- and 1.25-mm collimated sections accurately characterized the size of skull base defects in 15 (75%) of 20 patients. Of our 19 patients, 10 had MPR images based on 0.625-mm axial datasets. In this group, MPR images described 11 (92%) of 12 leak sites found at endoscopy and overestimated 2 of 11 cases by only 3 mm each. We speculate that this overestimation is probably because of demineralized and nearly dehiscent bone present along the edge of the skull base defect that remains imperceptible despite high-resolution imaging. In some cases, the skull base defect may have been minimally enlarged at endoscopy while the overlying mucosa was stripped away to fully expose the defect.

The discrepancy between CT and endoscopy in the 3 of 9 cases based on the 1.25-mm axial datasets is larger, with an average of 8 mm. A side-by-side comparison of MPR images based on 0.625- and 1.25-mm axial datasets demonstrates the

superior quality of the submillimeter dataset (Fig 6). Depiction of fine bony detail is clearly sharper with 0.625-mm collimation. The images from 1.25-mm collimation are noisier, and the margins of the skull base defect are more ambiguous. Accordingly, CT evaluation of the true margins of the osseous defects may suffer.

A limitation of our study was that analysis of imaging and surgical data was performed retrospectively, so MPR images were not directly compared with thin-section direct coronal CT or MR imaging. However, the MPR images correctly detected CSF leaks at a rate similar to what has been reported with the use of high-resolution direct coronal scans.[8,10] Increasing the dose of radiation by adding direct coronal CT to compare with MPR images would be difficult to justify, but repeating the study in a prospective fashion with submillimeter CT collimation in all patients would be of benefit. With near-isotropic imaging, the value of MPR imaging could be further explored. Measurements of skull base defects could be compared with intraoperative measurements in multiple planes.

Conclusion

High-resolution MPR images from thin-collimation axial CT reliably detected CSF leaks. Active manipulation of the dataset at the workstation was crucial in identifying these defects, especially the smaller and more subtle ones, as oblique images were evaluated. Imaging should be performed after a positive β_2-TF assay confirms that the rhinorrhea contains CSF. In this way, the positive and negative predictive value of CT will be improved. In the presence of multiple skull base defects, MR cisternography or CT cisternography should be considered to pinpoint the active leak. The use of cisternography, however, is surgeon dependent because experienced endoscopists can usually determine at the time of surgery if a defect is leaking. Finally, when compared with intraoperative interrogation, CT measurements of the skull base defects are accurate when submillimeter collimation is available.

References

1. Brodie HA. **Prophylactic antibiotics for posttraumatic cerebrospinal fluid fistulae. A meta-analysis.** *Arch Otolaryngol Head Neck Surg* 1997;123:749–52
2. McMains KC, Gross CW, Kountakis SE. **Endoscopic management of cerebrospinal fluid rhinorrhea.** *Laryngoscope* 2004;114:1833–37
3. Schlosser RJ, Bolger WE. **Nasal cerebrospinal fluid leaks: critical review and surgical considerations.** *Laryngoscope* 2004;114:255–65
4. Warnecke A, Averbeck T, Wurster U, et al. **Diagnostic relevance of beta2-transferrin for the detection of cerebrospinal fluid fistulas.** *Arch Otolaryngol Head Neck Surg* 2004;130:1178–84
5. Lloyd MN, Kimber PM, Burrows EH. **Post-traumatic cerebrospinal fluid rhinorrhoea: modern high-definition computed tomography is all that is required for the effective demonstration of the site of leakage.** *Clin Radiol* 1994;49:100–03
6. Shetty PG, Shroff MM, Fatterpekar GM, et al. **A retrospective analysis of spontaneous sphenoid sinus fistula: MR and CT findings.** *AJNR Am J Neuroradiol* 2000;21:337–42
7. Shetty PG, Shroff MM, Sahani DV, et al. **Evaluation of high-resolution CT and MR cisternography in the diagnosis of cerebrospinal fluid fistula.** *AJNR Am J Neuroradiol* 1998;19:633–39
8. Stone JA, Castillo M, Neelon B, et al. **Evaluation of CSF leaks: high-resolution CT compared with contrast-enhanced CT and radionuclide cisternography.** *AJNR Am J Neuroradiol* 1999;20:706–12
9. Prokop M. **General principles of MDCT.** *Eur J Radiol* 2003;45 Suppl 1:S4–10
10. Honda O, Johkoh T, Yamamoto S, et al. **Comparison of quality of multiplanar reconstructions and direct coronal multidetector CT scans of the lung.** *AJR Am J Roentgenol* 2002;179:875–79
11. Tabaee A, Kassenoff TL, Kacker A, et al. **The efficacy of computer assisted surgery in the endoscopic management of cerebrospinal fluid rhinorrhea.** *Otolaryngol Head Neck Surg* 2005;133:936–43
12. Kirtane MV, Gautham K, Upadhyaya SR. **Endoscopic CSF rhinorrhea closure: our experience in 267 cases.** *Otolaryngol Head Neck Surg* 2005;132:208–12
13. Mirza S, Thaper A, McClelland L, et al. **Sinonasal cerebrospinal fluid leaks: management of 97 patients over 10 years.** *Laryngoscope* 2005;115:1774–77
14. Lee TJ, Huang CC, Chuang CC, et al. **Transnasal endoscopic repair of cerebrospinal fluid rhinorrhea and skull base defect: ten-year experience.** *Laryngoscope* 2004;114:1475–81